A Structural System Reliability Care Study of an Eight-leg Steel Jacket Offshore Production Platform

H. Nordal, Statoil, Stavanger, Norway
C.A. Cornell, Stanford University, Palo Alto, California
A. Karamchandani, Stanford University, Stanford, CA

ABSTRACT

The reliability of an idealized eight-leg, steel-frame offshore platform (excluding piling) under extreme wave loads has been estimated using structural system reliability analysis. Wave loads and member resistances were treated as random variables, and reliability calculations were performed under a variety of conditions using first order reliability methods. The issues examined include X-bracing versus K-bracing in the principal load-carrying bents, the effects of wave load variability on system redundancy, hypothetical damaged conditions that were simulated by removing selected frame members, and the adequacy of horizontal bracing to transfer loads between the frame bents. Deterministic static push-over analyses resulted in brittle system failure with no post first member failure capacity. Using proposed probabilistic redundancy measures the X-braced frame was found to be almost an order of magnitude better (more redundant) than the K-braced frame. The redundancy (as measured in this report) of both framing alternatives was found to increase as wave load variability decreased.

The ability of the structure to withstand damage (structural robustness) was measured by comparing the increased system failure probability for the damaged structure relative to that found for the intact structure. The framing alternatives were found to be comparably sensitive to damage. Calculated increase in failure probability is between one and two orders of magnitude.

NOMENCLATURE

A_x — cross sectional area

D — damaged state

d — outer diameter of member

d_i — inner diameter of member

E — modules of elasticity

F — force or force factor

f_y — mean yield stress

GM — Gulf of Mexico

I — intact state

k — buckling factor

NS — North Sea

P_f — probability of failure

R — resistance

β — safety index

ℓ — buckling length

η — post failure fraction of unfailed capacity

ρ — correlation factor

INTRODUCTION

In the recent years there has been a continuous development of system reliability methods capable of analyzing complex structural systems. In the present study, a method based upon the member-replacement technique as described in Guenard (1) has been applied in a case study of an eight-leg, steel-jacket platform.

The structure is shown in Fig. 1. It is an idealized structure in the sense that it is designed for the operational phase only, and thus does not include any added fabrication or installation steel. The importance of this should be kept in mind if an attempt is made to generalize the results of the study. Lateral forces are transferred to the piles primarily by the broadside diagonals and by the X-braces in the four vertical bents. At each level, horizontal X-braced panels transfer loads between the vertical bents. In our study we have estimated the reliability of the structure when subjected to extreme wave loads. We have focused on the behaviour of the four vertical bents (first X-braced then K-braced). The study is limited to their performance under the worst wave direction, namely a broadside wave from the south. Next we have varied the wave load variability and investigated its effect on the reliability of the two structural systems. Further we have evaluated the consequences of exogenously caused damage, and finally examined the behaviour of the horizontal X-braces that transfer loads between the vertical bents. For the wave direction analyzed the horizontal X-panels are almost unloaded in the intact structure.

The structure has previously been studied using a deterministic approach by Lloyd and Clawson (2). It was therefore possible to concentrate effort on probabilistic aspects such as uncertainty models for the environment and the structure (member capacities) and in particular on the system reliability analysis.

ANALYSIS METHOD

A brief description of the analysis method is given below. A more general discussion of structural systems reliability analysis methods is given in Karamchandani (3). The reliability analysis computer program FAILUR is described in detail in Guenard (1). The analysis estimates the probability of system failure due to extreme wave loads. Failure is defined for each individual member of the structure by a failure function describing a limit state. A member fails if a limit state is reached. The limit state or failure function used for the truss members of the example jacket is the condition that the axial member force is equal to its elastic resistance. When a member fails its stiffness drops to zero, and the member force becomes a constant, equal to a post-failure fraction of its maximum capacity. (The details of the semi-brittle force-deformation behaviour assumed for the truss members of the structure is discussed later.)

The formal criterion for failure of the system is a major loss in stiffness as measured by the deflection at the center of the top of the structure. Practically the analysis of a particular path or sequence of member failures was stopped when the
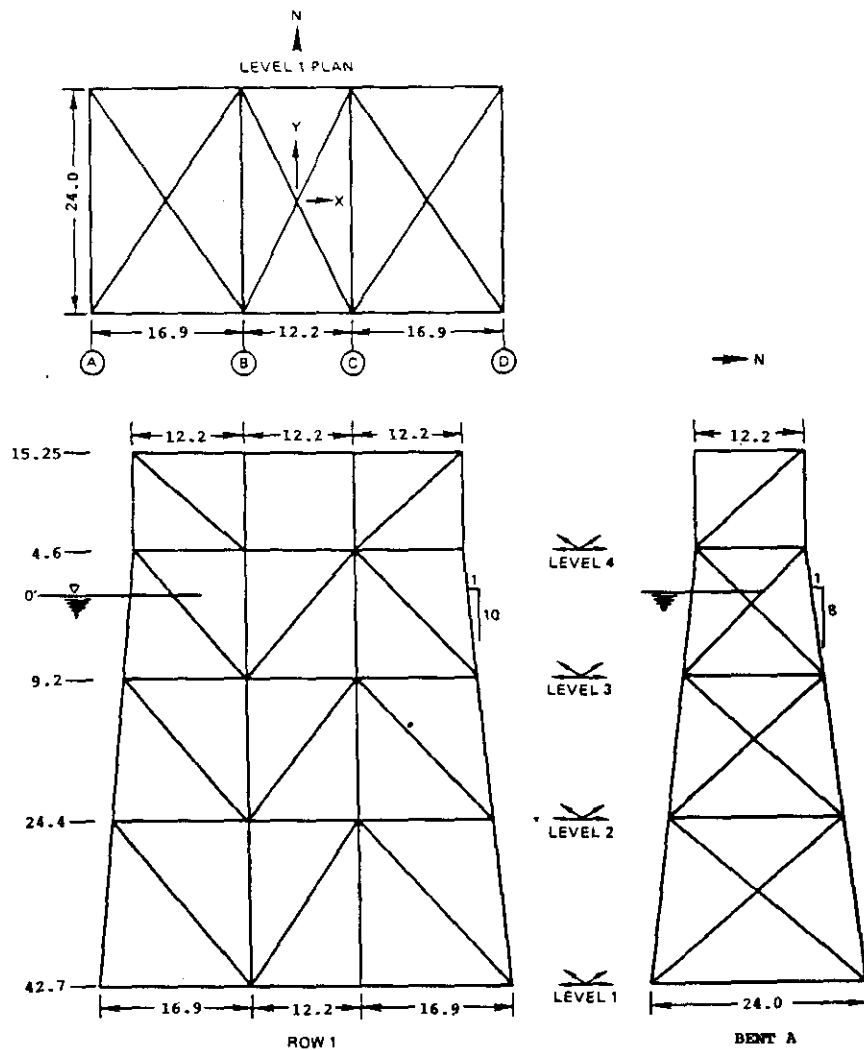
Fig. 1   General view of example structure. From Lloyd and Claw-
son (2). Dimensions in meter.

probability of the sequence stopped
decreasing; this was usually after 4
to 6 members in the structure had
failed. Failure of the system can be
defined in terms of failures of its
members. Each sequence of member
failures which leads to system fail-
ure is called a "failure path"; the
probability of system failure is the
probability any such failure path
will occur. If all possible paths are
not included in the analysis, then
the result obtained is a lower bound
on the probability of system failure
(i.e. since some potential failure

paths are ignored, the true system
failure probability will be larger).
If, for any specific path, all the
member failures in the path are not
considered (i.e. an incomplete path),
then the probability of occurrence of
the path will be larger than the true
value and a system failure analysis
including all such incomplete paths
will result in an upper bound on the
probability of system failure. In the
extreme case, the lower bound could
be the probability of occurrence of
any one particular complete sequence,
and the upper bound could be the

probability that any member fails in the intact structure (i.e. in each path only the first member failure is considered and all further failures are ignored). Because of approximations made, the "lower bound" used cannot, strictly speaking, be proved except under special conditions, e.g. pure elastic-plastic behaviour.

For most realistic structures, there are a large number of possible failure paths. Hence a search technique has to be used to identify the important paths (i.e. paths which have a high probability of occurrence). In Guenard (1), a branch-and-bound technique to identify the most important failure path has been described. In this technique the first step in to investigate the probability that a failure will occur in the intact structure. For each member i, the probability that the member fails, P (member i fails in the the intact structure) is computed. Note; this is also the probability that a damaged state with member i failed is reached. Let member i, be the member with the largest probability of failure. Hence, the damaged state associated with member i, failed is the most likely to occur damaged state. Focus now shifts to this damaged state. The next step is to investigate the probability of subsequent failures. The probability that a subsequent damaged state with member i, and j failed occurs is P (member i, fails in the intact structure and member j fails in a damaged structure with member i, failed). Once this has been calculated for all surviving members, the focus shifts to the currently most likely damaged state. This could be either a damaged state

with just one member failed or a damaged state with two failed members (i.e., member i, and another member j). Subsequent failures in this most likely damaged state are investigated next. The procedure continues until the damaged state being focused on is a collapse state (i.e. a damaged state in which the system is considered to be failed). The sequence of failures leading to this damaged state is the most likely failure path. This is guaranteed because of the unique "look-back" feature in this algorithm. This procedure can be continued (i.e., looking at the next most likely to occur damaged state) to generate other important failure paths.

The computer program "FAILUR" has an option to automatically perform such a branc-and-bound search for the most important paths. In the idealized structure being studied, however, because many of the critical member (such as the X-braces in the critical bents) have very similar failure probabilities, the total number of damaged states to be investigated is very large (i.e. many alternative damaged states with similar probabilities of occurrence exist) and the computation time (and memory requirement) is too large to be practically feasible on a minicomputer. Therefore in this study the potential failure paths were identified using manual searches. Although the paths identified using such manual searches are not guaranteed to be the most important paths, past experience indicates that this will usually be the case. In fact in many cases, in the manual search, only one important failure path was identified. As discussed below, this is usually sufficient to describe the

system behaviour in the system reli-
ability sense.

The results of the searches are
presented in the form of failure
trees. In these trees, the nodes
represent damaged states of the
structure and the branches enervating
from a node represent member failures
in the corresponding damaged struc-
tures. The notation used in these
failure trees is explained in Fig. 2.

In addition to the probabilis-
tic analysis a set of analysis with
member resistances deterministically
equal to the mean resistance was
carried out. They were used to com-
pare with the more advanced struc-
tural model of Lloyd and Clawson (2),
and to compare with the probabilistic
analysis performed. For example, one
can compute the probability that the
random loads will exceed simply the
deterministic system resistance.

MODELLING OF THE CASE STUDY

Structural Model

The structural model was made
as simple as could be justified. In
order to concentrate on the probabi-
listic aspects of the study, the
results of Lloyd and Clawson (2) were
used as guidance in identifying the
dominant structural behaviour.
In their study, Lloyd and
Clawson report the structure to glob-
ally act like a truss, and further
that the main contribution to frame
action in the structure is due to the
direct wave loads on the members in
and below the wave zone. As a conse-
quence it was anticipated that global
behaviour could be modelled by a
truss element model if the wave loads
are treated as concentrated joint
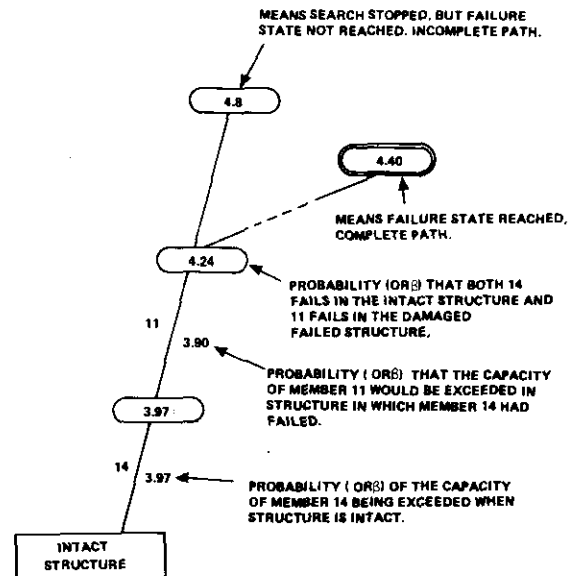loads. These assumptions lead to a

Fig. 2   Failure tree notation

space truss model representation of
the structure consisting of 216 truss
elements and 67 nodes. The foundation
is rigid.

The structure was designed
according to the API guidelines using
all X-braces. Dimensions of the ver-
tical X-bents are given in Fig. 3.
Some members were sized simply accor-
ding to general requirements such as
maximum member slenderness, minimum
diameter, and minimum wall thickness.
Examples of such members are the
horizontal X-panels. The dimensions
of these members would normally have
been dictated by some temporary
design condition prior to the opera-
tional phase of the structure. How-
ever, for this example study no such
condition was explicitly considered.

The API recommended k-factors
used to design the structure are
given in Table I. Based on recent
testing experience, more realistic
values of k's were recommended by
engineers at Exxon for calculating
the mean resistance of the jacket

Table I. Table of buckling lengths, ℓ , and reduction factors k.
API design values and assumed mean values.

Member type	Design k , ℓ	Used in this study to predict mean capacity k , ℓ
X-brace	0.9 , ℓ/2	0.5 , ℓ/2
K-brace	0.8 , ℓ	0.7 , ℓ
Diagonal brace	0.8 , ℓ	0.5 , ℓ
Leg	1.0 , ℓ	0.5 , ℓ
Horizontal leg to leg brace	0.7 , ℓ	0.5 , ℓ

* ℓ is for a brace the length along the brace from leg to leg.

members. These k-factors are also given in Table I. Note that the k-factor used for X-braces implies that the compression members are fully supported with respect to buckling out of plane by the intersecting tension member.

As part of this study the structure was redesigned with vertical X-braces replaced by K's. The vertical bents of this structure is shown in Fig. 4. The K-braces were sized by matching the values of only the axial force term in the API-guideline unity checks with the corresponding terms in the original X-braced design. Other matching criteria might have been used, e.g., equal weight, equal total unity check or equal reliability level. The combination of the chosen matching rule and the k-factor values had a profound influence, as will be seen below.

The elevation of the horizontal framing was not changed, the batter of the members in the K-brace is thus twice the batter of the X's. This is one source of difficulty in the comparison. The K-braces may not be typi-

cal in this respect.

The force-deformation diagram shown in Fig. 5 was applied to describe the member properties. In this semi-brittle model, the member force increases elastically to the member capacity or resistance. After failure, i.e. if the axial deformation in the element is increased beyond its failure value, the element force abruptly drops to a fraction, η , of its unfailed capacity. For this application a deterministic value of $\eta = 0.4$ was used for members failing in compression and $\eta = 1.0$ for tension failure. In other words we assumed ductile tension failure behaviour, maintaining the failure load, and an abrupt drop to 40 % capacity when failing in compression. The validity of these assumptions is discussed in the light of the analysis results.

In a probabilistic context the random member properties are described by a mean resistance, a coefficient of variation (COV) and a probability distribution. In contrast to the design capacities taken from codes, which include some conservatism, the

Fig. 3   Dimensions of X-braced vertical bents
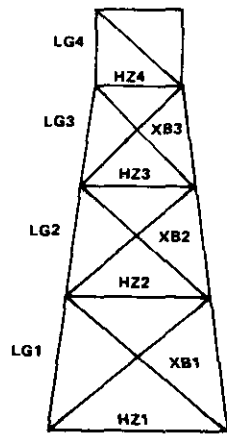
MEMBER GROUP	DIAMETER in cm (inch)	THICKNESS in cm (inch)
HZ1	61 (24)	0.95 (0.375)
HZ2	51 (20)	0.95 (0.375)
HZ3	41 (16	0.95 (0.375)
HZ4	36 (14)	0.95 (0.375)
XB1	51 (20)	1.27 (0.500)
XB2	46 (18)	1.27 (0.500)
XB3	36 (14)	1.59 (0.625)
LG1	100 (39.25)	4.76 (1.875)
LG2	100 (39.25)	3.49 (1.375)
LG3	100 (39.25)	3.49 (1.375)
LG4	100 (39.25)	1.91 (0.750)

Fig. 4   Dimensions of K-braced vertical bents
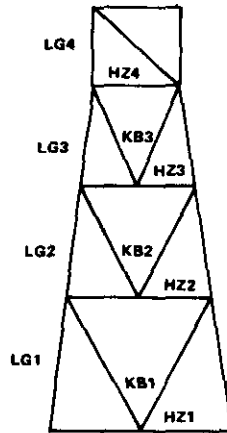
MEMBER GROUP	DIAMETER in cm (inch)	THICKNESS in cm (inch)
HZ1	61 (24)	2.86 (1.125)
HZ2	51 (20)	1.91 (0.750)
HZ3	41 (16)	1.91 (0.750)
HZ4	36 (14)	0.95 (0.375)
KB1	61 (24)	1.27 (0.500)
KB2	56 (22)	1.27 (0.500)
KB3	41 (16)	1.27 (0.500)
LG1	100 (39.25)	4.76 (1.875)
LG2	100 (39.25)	3.49 (1.375)
LG3	100 (39.25)	3.49 (1.375)
LG4	100 (39.25)	1.91 (0.750)

mean resistances are best estimates of the "real" capacity.

The AISC formula given below was used for the capacity of compression members. Note that for our application the code safety factor was removed.

$$R_c = 0.85 f_y A_x (1 - \frac{(k\ell/r)^2}{2C_c^2})$$

$$C_c = \sqrt{\frac{2 \pi^2 E}{f_y}}$$

$$r = \sqrt{\frac{d^2 + d_i^2}{4}}$$

A 15 % reduction has been introduced in the resistances (the 0.85 factor) to compensate for the neglected moments induced by frame action. The tension capacity was calculated as

$$R_T = 0.85 f_y A_x$$

which is conservative due to the 15 % reduction factor.

In general the members in the example structure had low slenderness ratios resulting in low reduction in the compression capacities due to buckling.
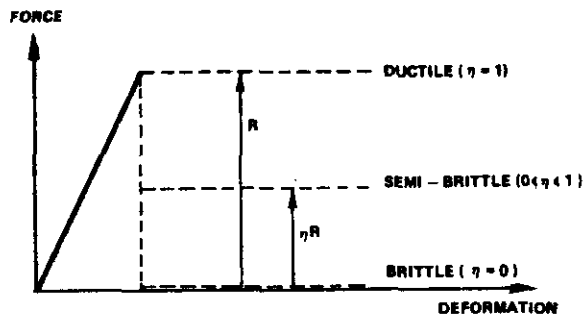
Fig. 5   Member force deformation model

The member resistances were assumed to be lognormally distributed, with a coefficient of variation (COV) of 10% for the tension capacity and 13 % for the compression capacities. The COV's are based upon work presented by Moses (4).

Environmental and Structural Load

Gravity and environmental loads acting on the jacket structure were in the computer program modelled as two fixed patterns each being scaled by a random variable. One load pattern is used for lateral environmental (wave) loads and one for vertical dead load, Guenard (1). The wave load pattern used is based on the set of forces acting on the structure due to the 19.2 meter (63 foot), 100-year design wave. This pattern is input as nodal forces to be consistent with the truss modelling of the structure.

Wave loads acting on the structure are basically drag dominated. The wave height, H, to base shear, F, transformation can therefore for our application be approximated by:

$$F = C \ H^X = F_{19}(H/19)^X = F_{19} \ x \ F_{\ell\ell}$$

with $x = 2.0$ to 2.2, C a constant, F_{19} is the base shear associated with the 19.2 meter wave pattern of forces, and $F_{\ell\ell}$ is a scale factor dependent on H.

In using this load model, i.e. scaling of the fixed load pattern, one should keep in mind the danger of scaling beyond realistic values, both with respect to realistically occurring waves and associated velocity fields and with respect to changed structural geometry due to surface effects. In particular the wave height should be compared with the actual deck elevation. In our example study, the deck elevation is 15.25 meters (50 feet) above mean sea level. Consequently for wave heights above about 30.5 meters (100 feet) the structure will be unconservatively analysed because we neglect the sudden increase in wave load when the deck is hit. (The importance of this assumption is under current investigation.)

$F_{\ell\ell}$ is a function of the wave height, consequently the mean, COV and probability distribution of $F_{\ell\ell}$ are all indirectly given when these are known for the wave height. The wave loads are assumed here to follow a lognormal distribution, Moses (4). As discussed there, $F_{\ell\ell}$ also includes, in addition to H, a random factor to describe the uncertainty in predicting the forces (base shear) given the wave height. Background data for the COV values used can be found in Moses (4) and Anderson et al (5). Two sets of $F_{\ell\ell}$ are used in this study, one representing a typical Gulf of Mexico (GM) case (our base case), and one a North Sea (NS) case, see Table II. The GM case is also referred to as the high-COV case as opposed to the low-COV case of the NS. This higher COV is due in part to the hurricane risk in the GM. As both cases are scaled to have the same 100-year wave, (0.99 fractile), the mean of the NS case is higher than the GM case due to the

200

lower COV of the former case.

The values given in Table II are lifetime values, i.e. representing the mean and COV of the forces induced by the extreme wave occurring in the (20 year) lifetime of the structure. This results in the failure probabilities discussed in this study being lifetime probabilities.

Table II. Wave load scaling factor $F_{\ell\ell}$. Means and coefficients of variation.

	Mean	COV
Gulf of Mexico, GM	0.75	0.37
North Sea, NS	0.85	0.23

Included in the forces, F_{63}, is also a factor of 1.6 to account approximately for loads due to miscellaneous appurtenances (conductors, etc).

DISCUSSION OF RESULTS

General Structural Behaviour of Intact Structure

When subject to a broadside wave load (south direction), the structure behaves basically as four identical parallel bents. Any asymmetry in the load are distributed by the horizontal frames (X-braced). The capacity of the structure to sustain lateral load is dictated by the capacity of the framing system in the vertical bents. The vertical bents are almost identical with respect to size and dimension, resulting in a well balanced structure. As will be discussed later this behaviour is important to keep in mind when evaluating the results obtained in the probabilistic analysis. More realistic structures will in many

cases include additional steel and framing dictated by design requirements for phases prior to operation, and will thus have member capacities that are more unbalanced, with respect to environmental loads.

X-braced Versus K-braced Vertical Bents in the Intact Structure.

X-bracedvertical bents. The base case studied was the intact structure with X-braced vertical bents in a Gulf of Mexico type environment. The general structural behaviour discussed above was observed. The two inner bents were virtually equally loaded, and the end bent were also significantly loaded. In addition the horizontal framing system was stiff enough to transfer forces effectively from one bent to another in case of failure and stiffness loss. Because of the low values of slenderness ratios $(k\ell/r)$, the capacity reduction due to buckling effects in the compression members was small. However, together with the compression loads induced by the gravity load in both members of the X's, it makes the compression members to fail first.

In the deterministic analysis this uniformity in load and capacities lead to a brittle system failure. If a post-buckling capacity of only 40 % ($\eta = 0.4$) is assumed for the semi-brittle compression members, the structure cannot sustain the force redistribution following failure of first compression member and collapses without load increase. Even with a ductile compression member assumption ($\eta = 1.0$), the deterministic system failure load is only 5 % larger than the first-member failure load. For the X-braced structure the

201

"correct" answer is somewhere between these limits, a more accurate compression member model would predict only a gradual reduction in member force with increased deformation. The consequence is that the system has very little, if any, overload redundancy as measured by post-first-member-failure capacity.

In the $\eta = 0.4$ deterministic analysis of the base case, failure occurred at an ultimate lateral capacity of 38300 kN (8600 kips). For comparison of results to follow, the probability of the load exceeding this deterministic capacity is 1.0×10^{-5} and corresponding safety index $\beta = 4.28$. This gives a Reserve Strength Factor (REF) defined as the ratio of environmental load at collapse (undamaged) to design environmental load of 3.3 to 3.45, comparing well with the REF = 3.5 reported by Lloyd and Clawson (2) based on a more advanced structural analysis.

In the probabilistic systems analysis performed here, we take account of the probability of lower or higher than average member resistances in addition to the load variability. However, for the analysis case with the large environmental load COV, the resistance COV is relatively small. The failure tree developed for the base case is shown in Fig. 6 with the notation from Fig. 2 and element numbers from Fig. 7. Based on an earlier preliminary analysis, only 40 of the 216 members were formally treated in the probabilistic study, the remaining members have negligible chance of failing.

Only one complete failure path representing structure collapses is shown. This is the most probable failure path with safety index $\beta = 4.4$. The path starts with failure in the most likely to fail member in the intact structure and involves failure in all members of the vertical X-braces at the second level bay.

The other branches in the tree are incomplete failure paths. They all have safety index comparable to that of the most probable failure path. The search in these branches were stopped when the increase in safety index by going one step further into the tree was small. In the X-braced structure this occurred after 4 members at the same bay level had failed. A general observation from the failure tree is that the mechanisms leading to system failure are failure of all members in the vertical X-braces at one of the bay levels.

The tree in Fig. 6 shows why the automatic search option in the computer program was ineffective for this structure. Following the automatic search criteria of searching for the "node" with the lowest β, all "nodes" in the tree with safety index lower than 4.4 will be developed prior to the final node in the most probable failure path. In particular this leads to that may of the failure paths developed includes the same members with only slightly different member failure sequence and nearly the same safety index. It can be shown that only a small error is introduced in the calculation of the system safety index by ignoring one of these failure paths.

The results of the probabilistic analysis of the base case are summarized in Table III, (case X-I-GM). Second vertical column in
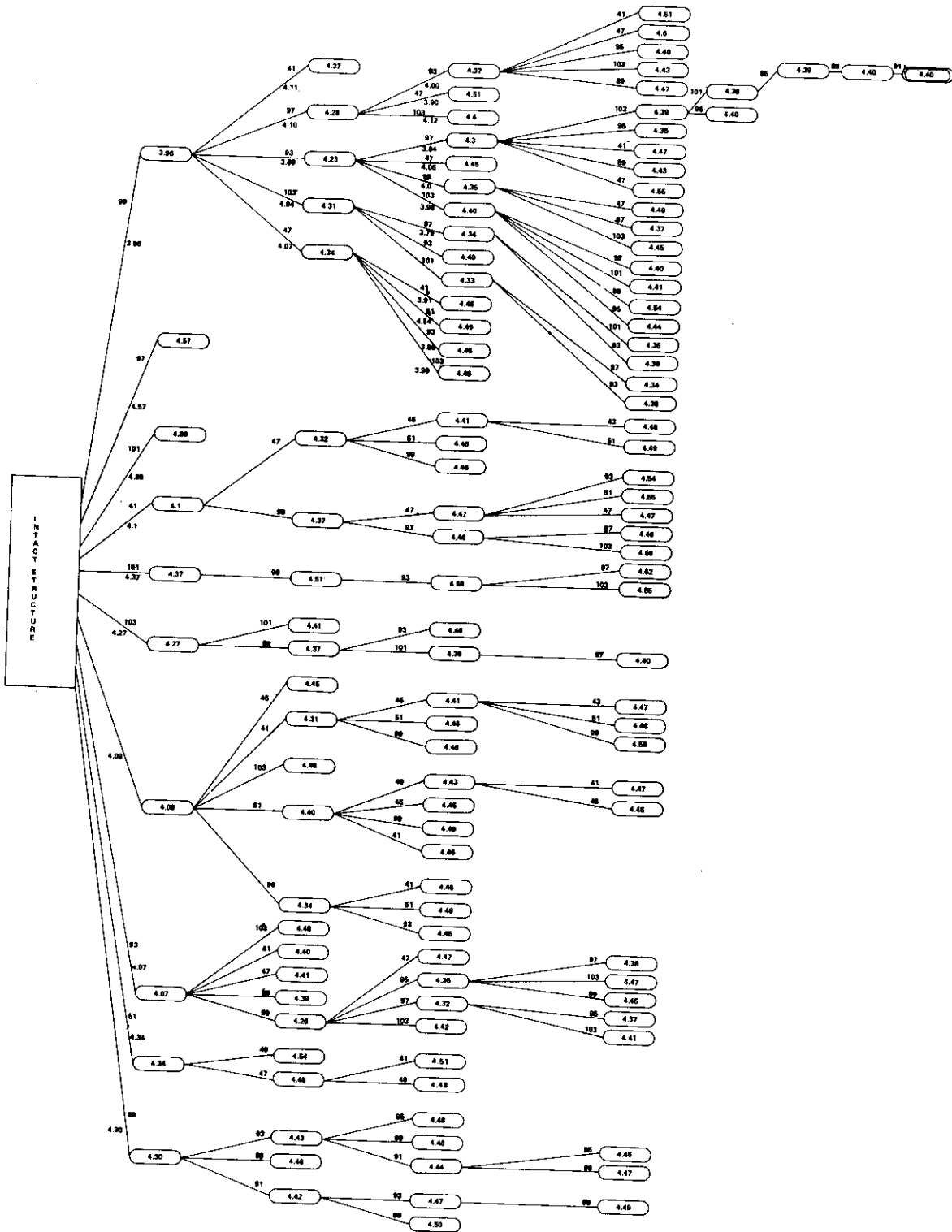
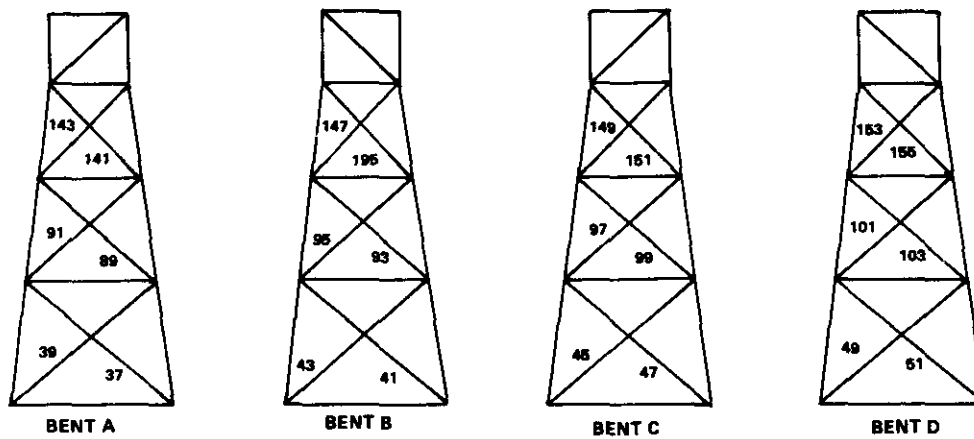Fig. 6   Failure tree, base case X-I-GM

Fig 7 X-braced vertical bents. Member numbering.

the table gives the safety index (and corresponding probability of failure) of the Most-Likely-To-Fail member (MLTF). This is the lowest index found when comparing all members in the intact structure. Third column gives the safety index calculated from the union of first member failures. It represents the probability that at least one (i.e. any) of the members in the system might fail in the intact structure. In the fourth column, the most probable failure path safety index is given, and finally the fifth column gives the system safety index representing the probability of failure or collapse of the entire structural system.

The MLTF-member in the base case is the member loaded in compression at the second level bay of the most heavily loaded inner bent. In calculating the union of any first member failure, it was noted that a union of only the 6-8 most likely members of the vertical X-braces in the intact structure gives approximately the same results as the union of all members. This indicates that these few members which all are loaded in compression by the wave

load, govern the any-first-member-failure probability. The system safety index is 4.2 corresponding to a failure probability of 1.3×10^{-5}. This is about an order of magnitude less than the probability that a member will fail in the structure. Probabilistically, the likelihood that the system will fail given that a member fails is therefore about 10 % implying in effect a kind of redundancy not detected in the deterministic analysis.

The base case structure was reanalyzed with wave load variability representing a North Sea environment. The results are summarized as case X-I-NS in Table III. Comparing the two cases, one sees first the lower probability of first member and system failure in the NS case. Recall however that the mean loads are scaled such that the 100 year design wave height is the same in both cases. Because of its lower COV, the mean scaled load is 13 % higher in the NS case. The higher β is a result of the lower COV and the high REF. More important for our purpose we see a larger difference between the union of any first member β and the system β

204

Table III   Table of results. Numbers are safety index, unclamped, and corresponding probabilities of failure, clamped.

Case	MLTF	Union of any 1st failure	Most likely failure path	System failure
X-I-GM	$3.96(3.7\times10^{-5})$	$3.71(11\times10^{-5})$	$4.40(5.4\times10^{-6})$	$4.20(1.3\times10^{-5})$
X-I-NS	$5.10(1.0\times10^{-7})$	$4.97(3.0\times10^{-7})$	$5.98(1.0\times10^{-9})$	$5.94(1.1\times10^{-6})$
K-I-GM	$3.06(1.1\times10^{-3})$	$2.87(2.0\times10^{-3})$	$3.17(0.8\times10^{-3})$	$3.03(1.3\times10^{-3})$
K-I-NS	$3.84(1.6\times10^{-5})$	$3.75(8.8\times10^{-5})$	$4.09(5.4\times10^{-6})$	$3.95(3.9\times10^{-5})$
X-D-GM(A)	$3.15(8.2\times10^{-4})$	$3.11(9.7\times10^{-4})$	$3.52(2.2\times10^{-4})$	$3.50(2.3\times10^{-4})$
X-D-GM(B)	$2.71(3.4\times10^{-3})$	$2.71(3.4\times10^{-3})$	$3.42(3.2\times10^{-4})$	$3.40(3.4\times10^{-4})$
X-D-GM(C)	$2.26(1.2\times10^{-2})$	$2.25(1.2\times10^{-2})$	$3.20(6.9\times10^{-4})$	$3.19(7.0\times10^{-4})$
K-D-GM	$1.52(6.4\times10^{-2})$	$1.52(6.4\times10^{-2})$	$1.64(5.1\times10^{-2})$	$1.62(5.3\times10^{-2})$

(or failure probabilities) in the NS case. In other words the "system-effect" is larger in the lower-load-COV case, NS. We shall discuss this point further below.

For both the GM and NS analyses, as well as for the deterministic case, a system failure mode tends to develop at the same bay level in all four vertical X-braced bents. Due to this localization vertically and due to the previously discussed load-capacity uniformity, this system can be compared to a simple ideal parallel system consisting of four semi-brittle components. Such a system is discussed in Guenard (1). His results are presented in Figs. 8 through 11.

Approximate analysis of this large structure via this simple ideal model can be useful particularly in terms of faciliating a more general perspective. For our application we interpret $n = 1$ (where n is the number of components) in the figures to represent the system safety, and $n = 4$ to represent the system safety. The "components" for our structure are now (two-member) X-braces. Consider first the characteristics of this equivalent component. Using the tension capacity (t.c) of a member in the X-brace as a unit reference, the compression capacity is 0.93 t.c. At failure of the compression member, the capacity of both members acting together, i.e., the ultimate capacity
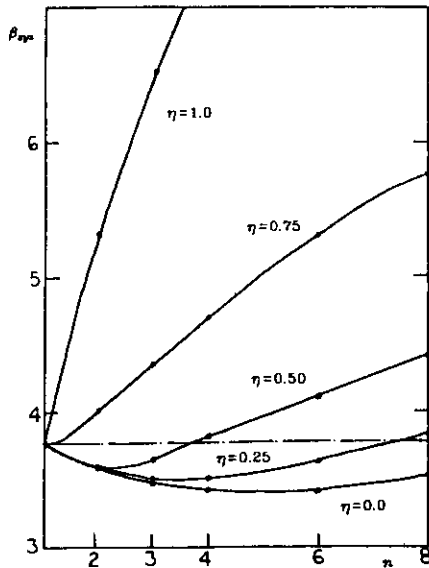
Fig. 6   Results cf ideal parallel
          system analysis
          ($\rho_R = 0$)

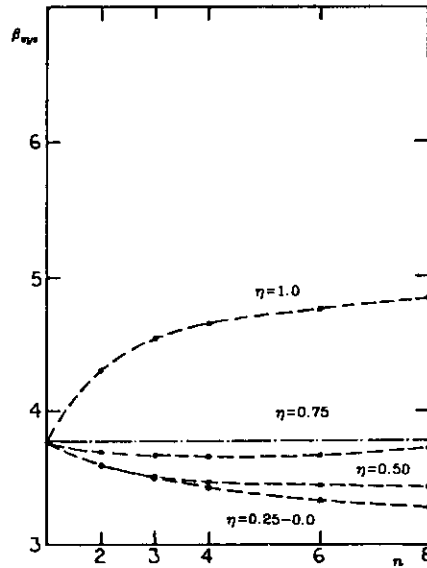
Fig. 9   Results of ideal parallel
          system analysis
          ($\rho_R = 0.50$)

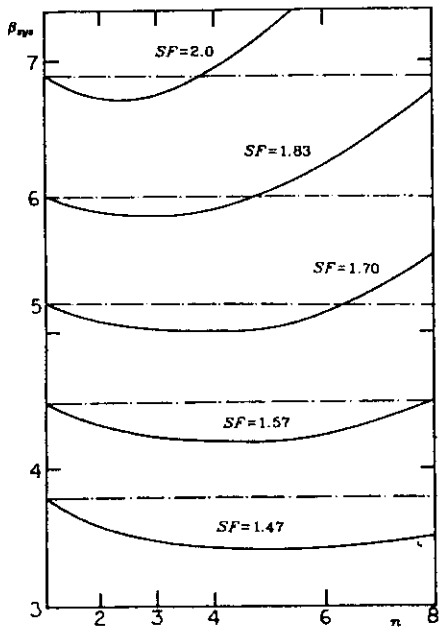

Fig. 10   Influence of SF on the
          redundancy of the
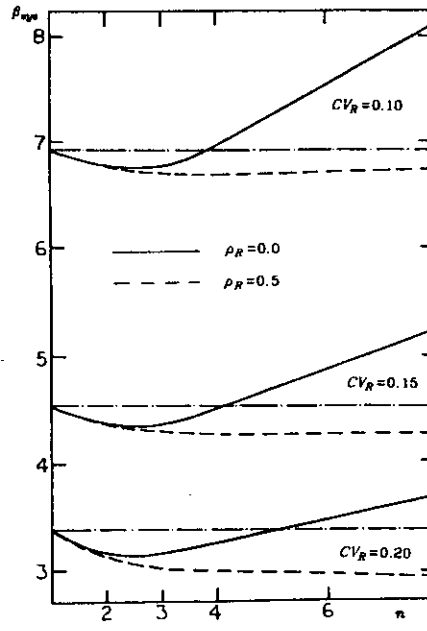   brittle ideal parallel
          system ($CV_R = 0.10$)

Fig. 11   Influence of CV_R on the
          redundancy of the
          brittle ideal parallel
          system (SF=2.0)

ρ_R – correlation between member resistances

SF   – safety factor = $\dfrac{nR}{L}$, with R common mean resistance and
       L load

CV_R – coefficient of variation common to all resistance
       variables

n   – number of components in parallel

206

of the X-brace is: $2 \times (0.93 \text{ t.c.}) = 1.86$ t.c. After failure of both members the residual strength of the X-brace is (with the ductile tension member and the 60 % reduction in the compression member capacity): $(0.4 \times 0.93 + 1.0)$ t.c. $= 1.37$ t.c. The post-failure capacity as a fraction of the ultimate capacity, η, is thus: $1.37/1.86 = 0.74$. Further, the load COV is 0.37 and 0.23 (for GM and NS, respectively), the net COV is found from $(0.37)^2 + (0.13)^2 = (0.39)^2$ and $(0.23)^2 + (0.13)^2 = (0.26)^2$ and the effective correlation between "component" safety margins is about 0.89 and 0.67, respectively. The effective correlation is measured here by the ratio of load variability to total variability.

$$\rho_{GM} = (0.37)^2 / ((0.37)^2 + (0.13)^2) = 0.89.$$

Unfortunately the parameter range considered in Guenard's case study, Figs. 8 through 11, does not cover our case. Study of the figures does, however, show general trends. Fig. 9 shows that in particular for higher correlation levels the benefits of low degrees of redundancy, i.e. $n = 2$ to 6, are not present unless n is high. The benefits increase, however, with higher β (Fig. 10) and with lower COV's, as we have when we compare the North Sea case to the Gulf of Mexico case. This simple ideal system representation does not of course capture the small but potentially important difference in mean resistance/load ratio that exist between bents, nor the effects of initial forces induced by vertical loads.

Several probabilistic measures of the redundancy of a system can be suggested. For example the difference between β_s (system) and β_a (any first member failure) perhaps divided by β_s is a β measure of the conditional reliability of the system given a first member failure. For a statically determinate system, $\beta_s = \beta_a$ and the difference is always zero. In the opposite extreme, for a system with extremely high redundancy β_s would be much larger than β_a and the difference would be approximately equal to β_s itself, i.e., the system is almost as reliable given a member failure as it is before. (Normalized by β_s the redundancy measure for this "perfectly" redundant system would be unity.)

With the results from Table III the (normalized) differences for the X-I-GM and the X-I-NS case, become respectively: 0.12 and 0.16 i.e., low values on the 0 to 1 scale. In contrast, from Fig. 8, we see ratios as high as 0.5 for parallel systems, even with a small number of parallel "members", provided they do not lose a significant portion of their failure load ($\eta = 1.0$ to 0.75), and provided ρ is small (close to zero). This last condition might apply in fatigue rather than extreme load situations.

A similar, but more direct measure of redundancy is the conditional probability of system failure given any first member failure. This is the ratio of the system failure probability to the first member failure probability. These ratios are 0.12 (X-I-GM) and 0.003 (X-I-NS).

For both redundancy measures we note that the system redundancy depends on the load characteristics as well as the structure itself. The redundancy measures for the structure are summarized in Table IV.

Table IV   Redundancy measures

Case	Redundancy measure 1[*]	Redundancy measure 2[**]
X-I-GM	0.12	0.12
X-I-NS	0.16	0.003
K-I-GM	0.05	0.7
K-I-NS	0.05	0.4

[*] Normalized safety index difference.
[**] System failure probability condi-
     tional to any first member fail-
     ure.
(See text for definitions)

The first member failure proba-
bility used above, is the probability
of any first-member failure. This
probability will be larger than the
most-likely-to-fail-first member
probability, because it represents
the probability of the union of all
possible first member failures. It
has the benefit of representing what
might be called "system complexity",
the more the number of highly
stressed members the larger this
probability will be relative to the
most likely member's failure proba-
bility. On the other hand high effec-
tive correlation as is induced here
by high load variability, will reduce
the difference between these two
first-member failure measures.

In this study the probability
of the union of all possible first-
member failures and the probability
of the union of all possible failure
paths are found not to be greatly
different from those associated with
most likely first member and most
likely failure path, owing to the
high load COV. The implication is

that the ratio of most-likely-
failure-path probability to most-
likely-first-member probability may
be a good estimate of the preferred
ratio; system probability to any
first-member-failure probability. For
the X-I-GM case the ratio of most-
likely-failure-path to MLTF-member is
0.14, which is very close to the
preferred, but more difficult to
calculate ratio above.

A final note: one should find a
redundancy definition that protects
against cases where highly likely
first member failures do not lead to
likely failure paths. These defini-
tions all require further thought.

The semi-brittle compression
member model used assumes a 60%
instantaneous drop in member force
following failure. Comparing this
load deflection behaviour, Fig. 5,
with experimental results, the full
(60 %) capacity reduction requires
axial member shortening of approxi-
mately 5 times the failure deforma-
tion. For the X-braced structure,
however, this deformation of a com-
pression member was found to be less
than two times the failure deforma-
tion prior to the corresponding ten-
sion member failure. At this level of
deformation, the remaining force in
the compression member is in the
order of 80 to 90 % of capacity. The
semi-brittle compression member model
may thus be quite conservative for
the X-braced system. A closer (but
somewhat unconservative) safety index
may be that associated with a per-
fectly ductile ($\eta = 1.0$) compression
member. For this value, in the GM
case, the safety index of the most
likely failure path increased from
4.40 to 4.75, viz-a-viz the first
member failure. (4.75 corresponds to
a probability of 1×10^{-6}). This

higher β_s implies a higher redundancy measure. The conditional probability above reduces for the X-I-GM case to 0.03.

We conclude that for X-braces, even in the large COV X-I-GM-case, with the preferred redundancy measure, i.e., the conditional probability of system failure given any first member failure, is between 0.03 to 0.12 and probably less than 10^{-1}.

K-braced Vertical Bents. In the K-braced structure, the predicted structural behaviour is in general not significantly changed compared to the X-braced case. In particular the uniformity and symmetry discussed above is still present. Therefore there is little or no post-first-member-failure system capacity. The deterministic semi-brittle structure fails upon failure of the first compression failure. Further, the post failure deformation of the compression members in the K-bays are large enough to make the semi-brittle representation less conservative compared to the X case. The $\eta = 1.0$ approximation would be much more unconservative for these K-bays. The results of the probabilistic analyses of the K-braced structure are summarized in Table III for the GM and NS-case (as case K-I-GM and K-I-NS respectively). Note the large drop, two orders of magnitude, in absolute reliability level for this system when compared to the results from the X-braced structure.

Referring back to the deterministically defined reserve strength factor, REF, this would be 2.3 for the K-braces structure, a significant reduction compared to the X-braced REF of 3.3. This drop is a consequence of several factors. Firstly we chose the dimensions of the K-braces so that the unity check with respect to axial loads were matched for the two framing alternatives when designed according to the API design guidelines. If we instead had chosen to match the total unity checks, the drop in reliability level would have been reduced by almost one order of magnitude. We could of course also have chosen some other matching criteria, for instance we could have aimed at matching the reliability levels of the two structural systems directly. The criteria chosen does however in principle represent what is thought of being more practical and realistic.

Given this API based matching criteria the reason for the resulting difference in reliability level can partly be explained deterministically. Utilizations in terms of axial load as a percentage of mean value axial capacity are given in Table V for the critical member in the two structures. Also given are the multiplication factors on the wave load necessary to reach 100 % utilization. The large difference in this factor and thus the reliability index is due to the relatively larger increase of the X-brace capacity to reach best estimate means as used in the reliability analysis (see Table I) and also due to the effect of the dead load reducing the available capacity of the X-brace to be utilized by lateral loads. The latter is a consequence of a broadly observed weakness of allowable stress based codes, that they lead to much lower overload margins in bracing members that are stressed only under extreme lateral loads such as waves, winds or seismic events. It should be noted that this effect would be even larger if the ratio of dead load to live load is

increased. One should keep in mind that K-braces analyzed herein are non-typical as the story heights in the structure were not changed. As a consequence the batter of the K-braces are twice that of the X-braces.

Table V   Utilization factors for critical X-brace and K-brace in vertical bents.

	Utilization Factor	Multip.factor on $F_{\ell\ell}$ to 100% Utilization
X-BRACE	0.27	4.36
K-BRACE	0.33	3.03

Repeating the analog to an ideal parallel system, as was done for the X-braces, the ultimate capacity of a K-brace "component" is: 2(0.8) t.c. = 1.6 t.c. (recall the larger $k\ell/r$ ratio). To maintain equilibrium after failure occurs in the compression member, the force in the tension member must also decrease, the post failure capacity of the brace system is therefore 0.4 x 1.6 t.c. = 0.64 t.c.. This results in postfailure capacity factor, $\eta = 0.4$. The effective correlation remains about 90 %. Referring to Fig. 9, the small reduction in system versus most-likely-first-member-failure probabilities found in the analysis is not surprising. In fact, with such a low η level one might not be surprised to find a four-bent system failure probability greater than that of an individual bent. It is also worth noting that in a K-braced bent,

when modelled as a truss, a mechanism is formed after first-member failure. The four-bent K-braced structure is thus more directly comparable with a four component ideal parallel system than the X-braced, as the latter requires failure in both members in a bent, i.e., a total of eight members in the four-bent structure to form a mechanism. This was however taken into account in this idealization when the X-brace was modelled as a "component".

The proposed redundancy measures for the structure with K-braced vertical bents are also given in Table IV. The X-braced structure had a conditional system probability of failure of about 10^{-1}, even in the high COV case. In contrast this probability is 0.7 for the K-braced. Deterministically we concluded that the K-brace would fail when a single member failed, whereas the X-braced system might carry a few percent more load (0 to 5 %, depending on the effectiveness of the remaining stiffness in the tension member in avoiding the drop to $\eta = 0.4$ of the compressive force at failure). System reliability analysis shows the X-braced system to have a redundancy measure about an order of magnitude better than that of the K (about 0.1 versus about 0.7). It is been observed in the study of ideal parallel system, e.g. Guenard (see Fig. 10, here) and Stahl and Geyer (6), that the absolute level of the reliability can influence the impact of redundancy. To test this issue we have analyzed a K-braced system with bracing capacities increased to give the same most-likely-first-member failure probability as the X-brace. The redundancy measure remained at 0.7. At the lower COV level the X-braced systems redundancy measure is

two orders of magnitude better. (Note again the dependance of the redundancy measure on the load COV). Concluding, the K-braced structure has only a small system redundancy effect even for the low COV case, in particular when compared to the effect in the X-braced structure.

X-braces Versus K-braces in a Damaged Structure

General. In order to assess the impact of damage on system reliability, the jacket was analysed with members removed. The damage may be caused by an accidental loading, fatigue or defects. In a deterministic framework Lloyd & Clawson (2) measure a structure's ability to sustain a member failure by its residual strength, defining Residual Resistance Factor (RIF) as the ratio of environmental load at collaps damaged to the environmental load at collaps undamaged. From a probabilistic viewpoint we will assess the system sensitivity to damage by comparing the increase in system failure probability in the damaged condition to that of the intact structure.

Only lifetime system safety indices have been calculated for the damaged structure. In a real project such information could be useful in the case of assessing the effect of undiscovered damaged, for instance, in connection with evaluating the necessity of inspection. In the event of known damage, one should however, obtain the annual β's as they would give useful information in determining if repair can be postponed to the following summer season, or if immediate action is required.

An important effect of damage to a tension member in a X-brace is that the buckling length of the adjacent compression member will increase, i.e., its capacity decreases. Also its deformation will increase causing the semi-brittle model ($\eta = 0.4$) to become less conservative. In the following, both options, i.e., with and without reduced compression member capacity, are discussed.

Damaged X-braced Vertical Bents. The single member damage thought to be most critical for the structure, is damage to the tension member in the outer X-bent. With this tension member damaged, the compression member in this bent is the one most likely to fail first. The results found for the case when the damaged member is assumed to be able to provide lateral support to this compression member are denoted X-D-GM(A) in Table III. The safety index representing failure in the first (or next) member is 3.15. This is lower than that of the same member in the intact case ($\beta = 4.28$), due to the increased utilization of the compression member. The probability of system failure under storm waves is 2.3×10^{-4} ($\beta = 3.50$). Recall that (under the same semi-brittle compression member assumptions) the system failure probability of the intact structure is 1.3×10^{-5}. The probability of storm induced failure has been increased by a factor of about 20 by the presence of a previously damaged member. This change is a measure of the system robustness with respect to some exogenously caused failure. (A statically determinate system would have a probability of failure of unity given damage; a "perfectly" robust system, one that was not effected by the loss of a member would have no increase in

211

system probability failure.)

If the damaged tension member is not able to support the compression member in the same bent, the buckling length of this member is doubled, and the compression capacity of the member is reduced by approximately 20 %. The system probability of failure is 3.4×10^{-4} (case X-D-GM(B) in Table III) implying a robustness factor of 25.

It is interesting to confirm, by comparing these two damaged structure cased, that "redundancy" as measured here (system versus first member failure) is related to there being non-uniformity in relative utilizations of members (or bents). In these two cases, the system capacity and probability of failure is about the same, but in the second case the remaining member in the damaged bent is initially higher loaded relative to its capacity implying a higher first-member failure probability.

In the event of a full end-bent bay being damaged (no load bearing/shear capacity), the wave load/shear acting on that bent will have to be transferred to the remaining bents via the horizontal X-braces above. In this structure the unsymmetry introduces a large shear force in the bent next to the damage. The probability of failure of the compression member in this bent is therefore relatively high, see Table III case X-D-GM(C). The remaining part of the structure, however, still has some capacity for load increase. Therefore this damage system displays strong redundancy with respect to wave induced failure as measured by the system failure probability conditional to failure in the MLTF member probability. The net

system robustness has decreased with a factor two compared to the only one member damaged system. With respect to the system failure probability of the intact structure, this is increased by a factor of 55.

The analysis showed that the horizontal X-brace still have sufficient capacity to almost certainly keep the failure path within the vertical bents and at the damaged level, but the horizontal X-brace do start to become potentially susceptible to failure. Further it was observed that as members fail in the vertical bents, the remaining "planes" (horizontal X-planes, broadside diagonals and unfailed vertical X-brace) have comparable utilizations and β 's.

Damaged Structure -K-braced Vertical Bents. In the K-braced structure damage was simulated by removing a member loaded in compression in an end bent. The results from the analysis are summarized in Table III case K-D-GM.

One should keep in mind that unlike the X-brace, which still would have one active member left, the bay in the one-member-damaged K-braced structure transfers no shear load. Comparing probability of system failure in the intact (GM) versus the damaged structure the system probability failure increased from about 1.3×10^{-3} intact to about 5.3×10^{-2}. This is an increase in wave-caused system failure probability of about 40 due to the exogenously damaged (removed) member. Note that this measure of system robustness is of the same order of magnitude as that of the X-braced system.

Role of Horizontal Bracing in the Structural System

The horizontal bracing in the jacket has been sized using designers' prerogatives rather than code criteria, as this bracing is basically unloaded in the intact structure during its operational phase. In a real structure the on-barge transportation loads would have determined the dimension of some of these members; this structure, however, has only been designed for the operational condition. For the structure with vertical X-braces, the horizontal braces were sized according to:

Minimum wall thickness,
    t = 0.95 cm (3/8 inch)
Diameter to thickness ratio,
    D/t < 60.

Furthermore the bracing configuration (X's) was apparently rather arbitrarily chosen. This sizing approach resulted in a rather stiff horizontal framing, with k ℓ/r = 35 and thus only 10 % reduction in compression versus tension strength.

Analysis of the intact structure subject to a south (broadside) wave, proved that the horizontal braces fulfilled their mission by efficiently transferring and levelling out loads between the four vertical bents. Even in the damaged and post-failure cases, the horizontals appeared to be strong enough both with respect to carrying forces and stiffnesswise. In fact they seemed to have surplus capacity in all cases.

In order to understand better the limit between excess and insufficient strength of the horizontal

frames, the horizontal X-braces were replaced by diagonals single diagonal members. The member dimensions, as given by the above rules, were not changed. The reliability analysis of this intact structure revealed that the dominant failure mode was not influenced by this reframing, and that the system probability of failure was hardly changed. The damaged case investigated again consisted of removal of a tension member in the end-bent at the critical level bay. Even for this case, the most likely failure mode appeared in the vertical X's. However, a "vertical" failure mode consisting of failure in the horizontal diagonals framing inwards from the damaged bent appeared as next most likely.

Concluding, the analysis of the structure showed that a horizontal framing consisting of only simple diagonals was sufficient to fulfil the structural requirements of this framing when the structure is subject to a broadside wave, that is, the horizontal framing did not contribute to a significantly higher system probability of failure in fact this probability would not have been lower if the horizontals were infinitely strong. If, on the other hand, the capacity of the horizontal framing system was reduced significantly further, its members would control the reliability of the damaged structure. (Note that this conclusion may not be valid for other wave approach directions).

CONCLUSIONS

The example structure has been analyzed for several cases including X and K braces, high and low load variability and intact versus damaged states. Through these analysis a

structural system reliability analysis method has been demonstrated. Some results are summarized in Table VI.

From these results it can be concluded that the X-braced framing in the structure is superior to the K-braced as designed. This holds both with respect to absolute safety level and redundancy, when both framing systems are designed according to API and compared on the basis of axial design unity checks. Deterministically, the reserve strength factor REF for the K-brace is 70 % of that for the X-brace. The corresponding increase in system probability of failure is larger than one order of magnitude.

The reason for this difference is twofold, firstly due to the relatively larger increase in capacity of the X-brace when comparing best estimate values to design values, and secondly indirectly due to the vertical loads (dead load) being carried by the X's and the resultant increase in lateral overload margin.

The X-braced structure showed a larger system redundancy effect than the K-braced. This is in particular evident in the low load variability case when the variability of member resistances become relatively more significant. With the suggested redundancy measure of probability of system failure conditional on first member failure, the redundancy of the X-braced structure is minimum 7 times that of the K-braced, even in the high load variability case.

The study showed that the redundancy is sensitive to the modelling of member post-failure behaviour. Further the redundancy will increase when the difference in capacity between compression versus tension forces is large. In the study this difference was probably underestimated.

Robustness of the structure with respect to damage is measured by the increase in system failure probability following damage (removal) of a critical member. With this measure no significant difference was found between the two systems. In other words although the individual X-brace has a higher absolute safety level and redundancy, the overall system behaviour is not dissimilar for the two systems.

The study has revealed some interesting aspects with respect to redundancy and robustness measures. In its intact state the structure has high uniformity in member utilization. This results in a low redundancy measure. Damage of a member results in non-uniformity in utilization in the remaining structure, and as a consequence higher redundancy.

The result is an apparent inconsistency in that a "well designed" structure, i.e., well balanced, highly-utilized-members, implies low redundancy. Does this imply that redundancy is not as a desirable quality? Does it imply that the measure introduced here is inappropriate, although it works for statically determinate systems? Or does it mean that "robustness" is what we are really more interested in, i.e., we would not like a major reduction in system reliability if the structure is locally damaged? These issues should be further discussed in the light of the improved measuring capabilities of system reliability analysis.

Table VI   Summary of study results.

GM = Gulf of Mexico (high load variability)

NS = North Sea (low load variability)

BRACE TYPE	PROB. OF FAILURE INTACT		REDUNDANCY MEASURE		PROB. OF FAILURE DAMAGED	ROBUST NESS MEASURE
	GM	NS	GM	NS	GM	GM
X	1.3×10^{-5}	1.1×10^{-6}	0.1	0.003	3.4×10^{-4}	25
K	1.3×10^{-3}	3.9×10^{-5}	0.7	0.4	5.3×10^{-2}	40

It is worth noting that a "real" platform, as opposed to the example structure, would be more non-uniform due to design requirements from phases prior to the inplace operational phase. Although unintentional this would result in higher post-first-member-failure system capacities and a more redundant behaviour.

The member replacement technique, which is the basis for the system reliability analysis, has proved to be an efficient tool in comparing alternative structural systems and their redundancy or robustness. However, areas with scope for improvement in the technique, as implemented in the computer program FAILUR, have been identified.

The most important are:

- More detailed/realistic mechanical modelling of post-failure compression member behaviour.
- Member behaviour under combined axial and moment loading.

- More sophisticated load pattern modelling with respect to scaling.
- Capabilities of "more intelligent" automatic generation of failure trees.

ACKNOWLEDGEMENT

Paul Pike and others at Exxon, and Robert Bea of PMB Systems for their personal contributions to the study.

REFERENCES

1. Y.F. Guenard:
   Application of System Reliability
   Analysis to Offshore Structures,
   John A. Blume Earthquake Eng.
   Center , Stanford Univ., Report
   No.71, Nov. 1984.

2. J.R. Lloyd and W.C. Clawson:
   "Reserve and residual strength of
   pile founded, offshore plat-
   forms", The Role of Design,
   Inspection and Redundancy in
   Marine Structural Reliability.
   Proceedings, National Academy
   Press, Washington DC, 1984.

3. A. Karamchandani, Structural
   System Reliability Analysis
   Methods, Department of Civil
   Engineering, Stanford University,
   Draft report to the joint indus-
   try project Offshore Structural
   Systems Reliability, Feb. 1987.

4. F. Moses: Development of Prelimi-
   nary Load and Resistance Design
   Document for Fixed Offshore
   Platforms, API-PRAC Project
   85-22, Case Inst. of Technology,
   Cleveland, Ohio, January 1981.

5. W.D. Anderson, M.N. Silbert and
   J.R. Lloyd, "Reliability Proce-
   dure for Fixed Offshore Plat-
   forms",
   Journal of Structural Division,
   ASCE Vol. 108, No. ST11, Nov.
   1982, pp. 2517-2538.

6. B. Stahl and J.F. Geyer, "Ulti-
   mate Strength Reliability of
   Tension Leg Platform Tendon Sys-
   tems", 17th Annual Offshore
   Technology Conference, Proceed-
   ings, Houston, OTC paper 4857,
   May, 1985.